Supporting Information

For

Nanoplastic stress drives cyanobacterial secondary metabolism and taste-and-odor production

Jia-Xin Liu [a], Meng-Xin Xu [a], Long-Hai Cao [a], Mei-Yan Liu [a], Xiao-Yu Liu [a], Jing-Ya Ma [a], Jian-Lu Duan [a], Zi-Han Lang [a], Xiao-Han Zhang [a, b], Shu-Guang Wang [a, b], Xian-Zheng Yuan [a, b, c], Fan-Ping Zhu [a, b, *].

[a] Shandong Key Laboratory of Environmental Processes and Health, School of Environmental Science and Engineering, Shandong University, Qingdao, Shandong 266237, P. R. China

[b] Shandong Key Laboratory of Synergistic Control of Complex Multi-Media Pollution, Shandong University, Qingdao, Shandong 266237, P. R. China

[c] Sino-French Research Institute for Ecology and Environment (ISFREE), Shandong University, Qingdao, Shandong 266237, P. R. China

Corresponding author:

Fan-Ping Zhu,

School of Environmental Science and Engineering, Shandong University

72 Rd. Binhai, Qingdao, Shandong 266237, P. R. China

E-mail:

zhufanping@sdu.edu.cn

This supporting information contains 5 texts, 5 tables and 19 figures.

Text S1: Method for Detecting Odorants.

The inlet and ion source were both was set at 250 °C. Helium carrier was supplied at 1 mL/min in splitless injection mode. The column oven temperature program was as follows: initial temperature held 30 °C for 5 minutes, increased to 100 °C at 30 °C/min and held for 1 min, then ramped to 120 °C at 1°C/min and held for 2 min, and finally raised to 250 °C at 40 °C/min with a final hold time of 0.67 min. The qualitative ions for GSM were m/z = 112 and 125, and for 2-MIB were m/z = 95 and 107.

Text S2: Methods for Characterizing the Morphology and Surface Properties of *M. aeruginosa* Cells

SEM:

After centrifuging PS-NH_2-treated *M. aeruginosa* (8000 rpm, 10 min), the supernatant was discarded, and the pellet was collected and washed twice with PBS. The cells were fixed overnight in 2.5% glutaraldehyde. Subsequently, the samples underwent gradient ethanol dehydration (30%, 50%, 70%, 80%, 90%, and 100%) and were dried in a critical point dryer. Scanning electron microscopy (SEM) was then used to examine the samples at 2.00 kV acceleration voltage. For AFM imaging, 20 mL of the algal suspension was centrifuged (8000 rpm, 10 min), washed twice with PBS, and fixed on positively charged slides.

AFM:

AFM (JRK NanoWizard 4, Bruker) with an MLCT probe (radius 20 nm) was used to calculate the Young's modulus via Hertz/Sneddon model fitting. Prior to the experiment, the probe was cleaned with ethanol and ultrapure water, and the probe's elastic constant was calibrated using the thermal noise method before imaging. All experiments were conducted at room temperature[1].

CLSM:

The distribution of PS-NH_2 in *M. aeruginosa* was observed using confocal laser scanning microscopy (CLSM) and Rayleigh scattering. The excitation and emission wavelengths for PS-NH_2 were 360 nm and 420 nm, respectively. Confocal imaging was performed using a laser scanning confocal microscope (LSM-880, ZEISS, Japan).

Text S3: Metabolomic of *M. aeruginosa*

The raw targeted LC-MS/MS data were processed using TraceFinder software (Thermo Fisher Scientific) for peak extraction and integration. To trace the intracellular carbon flux and validate the substrate overflow mechanism, we employed a targeted quantification strategy specifically focused on the methylerythritol phosphate (MEP) pathway.

A tiered strategy was employed for metabolite identification and quantification. For the terminal T&Os (GSM and 2-MIB), absolute quantification was rigorously performed by constructing specific calibration curves using authentic chemical standards, achieving the highest identification confidence (MSI Level 1). For the upstream precursors and key intermediates within the MEP pathway (e.g., pyruvate), relative quantification was conducted based on the normalized integrated peak areas. These intermediates were identified by matching their accurate precursor masses and specific MS/MS fragmentation patterns against public databases (such as HMDB and mzCloud), achieving an MSI Level 2 identification confidence.

Statistical analyses were performed using R software (version 4.4.2). Because our targeted assay specifically monitored the MEP pathway rather than the global metabolome, data evaluation focused on the fold-changes and statistical significance of these predefined intermediates. Significant differences between the control and PS-NH_2 exposure groups were determined using Student's t-test, with a p-value < 0.05 considered statistically significant. The quantitative variations of these targeted intermediates were then directly mapped onto the MEP pathway to explicitly delineate the stress-induced carbon reallocation.

Text S4: Transcriptomics of *M. aeruginosa*

Library construction and sequencing

Library preparation was performed using the Optimal Dual-mode mRNA Library Prep Kit (BGI-Shenzhen, China). Briefly, total RNA was treated to enrich mRNA using oligo (dT) magnetic beads. The enriched mRNA was fragmented into small pieces using fragmentation reagents under elevated temperature. First-strand cDNA was synthesized using random hexamer primers, followed by second-strand cDNA synthesis. The synthesized double-stranded cDNA underwent end-repair, and a single 'A' nucleotide was added to the 3' ends to facilitate adaptor ligation.

Following amplification via PCR and quality control, the library products were denatured to generate single-stranded DNA. These strands were cyclized to form single-stranded circular DNA libraries, with uncyclized linear DNA digested. The final circular libraries were amplified using phi29 DNA polymerase via rolling circle amplification (RCA) to generate DNA nanoballs (DNBs), each containing over 300 copies of the original molecule. The DNBs were loaded onto patterned nanoarrays, and pair-end reads (PE 100/150) were generated on the DNBSEQ platform (BGI-Shenzhen, China).

Bioinformatics analysis

Data filtering and quality control. Raw reads were filtered using SOAPnuke (v1.6.5) to remove low-quality data. The filtering criteria included the removal of reads containing sequencing adapters, reads with an unknown base ('N') ratio greater than 10%, and reads where low-quality bases (quality score ≤ 15) accounted for more than 50% of the read length. High-quality clean reads were obtained and stored in FASTQ format for downstream analysis.

Reference genome mapping. The clean reads were mapped to the *M. aeruginosa* reference genome (Assembly: GCA_002095975.1_ASM209597v1) using Bowtie2 (v2.4.5). PCC 7806 was selected as the reference because a complete genome for the experimental FACHB-905 strain was unavailable at the time of transcriptomic analysis,

and PCC 7806 serves as a well-annotated homologous strain. The high compatibility of this surrogate reference was empirically confirmed by an average genome mapping rate of 97.13% across all samples.

Gene expression quantification. The expression level of each gene was calculated utilizing RSEM (v1.3.1), which generated the raw read counts. To accurately assess relative gene expression and address potential systemic biases across samples, gene abundances were normalized and quantified as Transcripts Per Kilobase Million (TPM).

Differential expression analysis. Differential expression analysis between groups was performed using the DESeq2 R package. To ensure robust statistical testing, DESeq2 determines differential expression based on the negative binomial distribution utilizing the unnormalized raw read counts. The resulting P-values were adjusted using the Benjamini-Hochberg procedure to control the false discovery rate (FDR). Genes with an absolute log2(fold change) > 1 and an adjusted P-value < 0.05 were identified as significantly differentially expressed genes (DEGs).

Functional enrichment analysis. To explore the biological functions of the DEGs, Gene Ontology (GO) and Kyoto Encyclopedia of Genes and Genomes (KEGG) enrichment analyses were performed using the phyper function in R software. A P-value < 0.05 was used as the threshold to identify significantly enriched terms and pathways.

Text S5: Quantitative PCR (qPCR) Analysis Methods

The same RNA samples prepared for transcriptomic sequencing were utilized for qPCR validation. Briefly, (rRNA) was removed from total RNA by the sequencing provider (BGI-Shenzhen, China) using a DNA probe hybridization and RNase H digestion method. First-strand cDNA was then synthesized from the rRNA-depleted RNA using a PrimeScript™ RT reagent Kit with gDNA Eraser (TaKaRa, China), following the manufacturer's instructions. qPCR was performed using TB Green® Premix Ex Taq™ II (Takara) on a QuantStudio™ 5 System (Applied Biosystems). Gene-specific primers were designed using PrimerQuest, with amplicon sizes ranging from 17 to 22 bp (The specific primer sequences are shown in Table S3.). The amplification efficiencies for all primer pairs were evaluated and found to be within the range of 90%-110% ($R^2 > 0.99$).

The qPCR reaction mixture (20 μL) consisted of 10 μL of 2× TB Green Premix Ex Taq II, 0.8 μL of each primer (10 μM), 2 μL of diluted cDNA, and nuclease-free water. The thermal cycling conditions were as follows: initial denaturation at 95 °C for 30 s, followed by 40 cycles of 95 °C for 5 s and 60 °C for 30 s. Relative gene expression levels were calculated using the $2^{-\Delta\Delta Ct}$ method, with 16S rRNA serving as the internal reference for normalization. Three biological replicates and three technical replicates were performed for each sample.

Tab. S1: The composition of BG-11 and concentration of the ingredients in BG-11 are as follows.

Nutritional ingredients	Concentration
$NaNO_3$	1.5 g/L
K_2HPO_4	0.04 g/L
Na_2CO_3	0.02 g/L
$MgSO_4 \cdot 7H_2O$	0.075 g/L
$CaCl_2$	0.027 g/L
Na_2-EDTA	0.001 g/L
$FeNH_4$-citrate	0.006 g/L
Citric acid	0.006 g/L
Trace element	1mL/L

Tab. S2. Composition of Micronutrient Stock Solution

Nutritional ingredients	Concentration
H_3BO_3	2.86 g/L
$Co(NO_3)_2 \cdot 6H_2O$	0.0494 g/L
$MnCl_2 \cdot 4H_2O$	1.81 g/L
$ZnSO_4 \cdot 7H_2O$	0.222 g/L
$CuSO_4 \cdot 5H_2O$	0.079 g/L
Na_2MoO_4	0.391 g/L

Tab. S3. qPCR Primer Sequences

Gene	Primer Sequence (5' to 3')
16S-F	CCGTCAAATCAGGTTGCTTAAC
16S-R	ACCGATGTTCTTCCCAATCTC
MAE_16190-F	CGAAGAAACGATCGCCACTA
MAE_16190-R	CGCCACCGTGGAGAATATAA
MAE_56570-F	CGAAAGCCAAAGAGCCAAAG
MAE_56570-R	GACCGAATGGCGGTAATACA
MAE_14550-F	CTAGCCTACGCTTTCGAGTATG
MAE_14550-R	AAACCTGACCTCCCACTAAAC
MAE_62650-F	CGCCCGGTTGTCACTATTTA
MAE_62650-R	CCGGTCCATGCAGAAGAAA
MAE_48090-F	GCCGTCCGTACTCTCAAATATC
MAE_48090-R	CTGCTTGCCAGACAGTGTAA
chlE-F	TTTCCGTCTTTGCTACCCATAG
chlE-R	GCGCGAGCAGAGGTATTATT
crtB-F	ATCCAACCCTTTCGGGATATG
crtB-R	CACCCGATAGCAGTACAGTTT
glnA-F	GGTCGTTGGAATAGCGGTAAA
glnA-R	GAGAGGTATCGGTGGGACTAA
psbC-F	GTCCCAGAAACCCTGAAAGAT
psbC-R	GCAGGTGATGACCGAGAATAA
nifJ-F	GATCCCAAACCCGCAGATTAT
nifJ-R	GGCACTCGCGAACTTCATTA
rbcS-F	TTGCCCACCACAGTGAAA
rbcS-R	GCCTTCGTACTCCTCCATAAAG
BH695_2768-F	CTCGACGAAGATGTGCAGTTA
BH695_2768-R	GACGGGCGGAATTATAGGATAG
BH695_2612-F	TTGTTATCGGTGCGGTTGTG
BH695_2612-R	ACGATCGAGCTTGGAGAGATAG

Tab. S4. Differentially expressed genes

Gene name	Description
MAE_16190	DXP – IPP/DMAPP
MAE_56570	IPP – DMAPP
MAE_14550	IPP/DMAPP – GPP/FPP
MAE_62650	Pyruvate – DXP
MAE_48090	Pyruvate – IPP

Tab. S5. Differential metabolites

Target metabolite name	Description
Pyruvate	Pyruvate
DXP	1-deoxy-D-xylulose 5-phosphate
IPP	lsopentenyl diphosphate
GPP	Geranyl diphosphate
FPP	Farnesyl diphosphate
GSM	Geosmin
2-MIB	2-methylisoborneol

Supplementary Figures

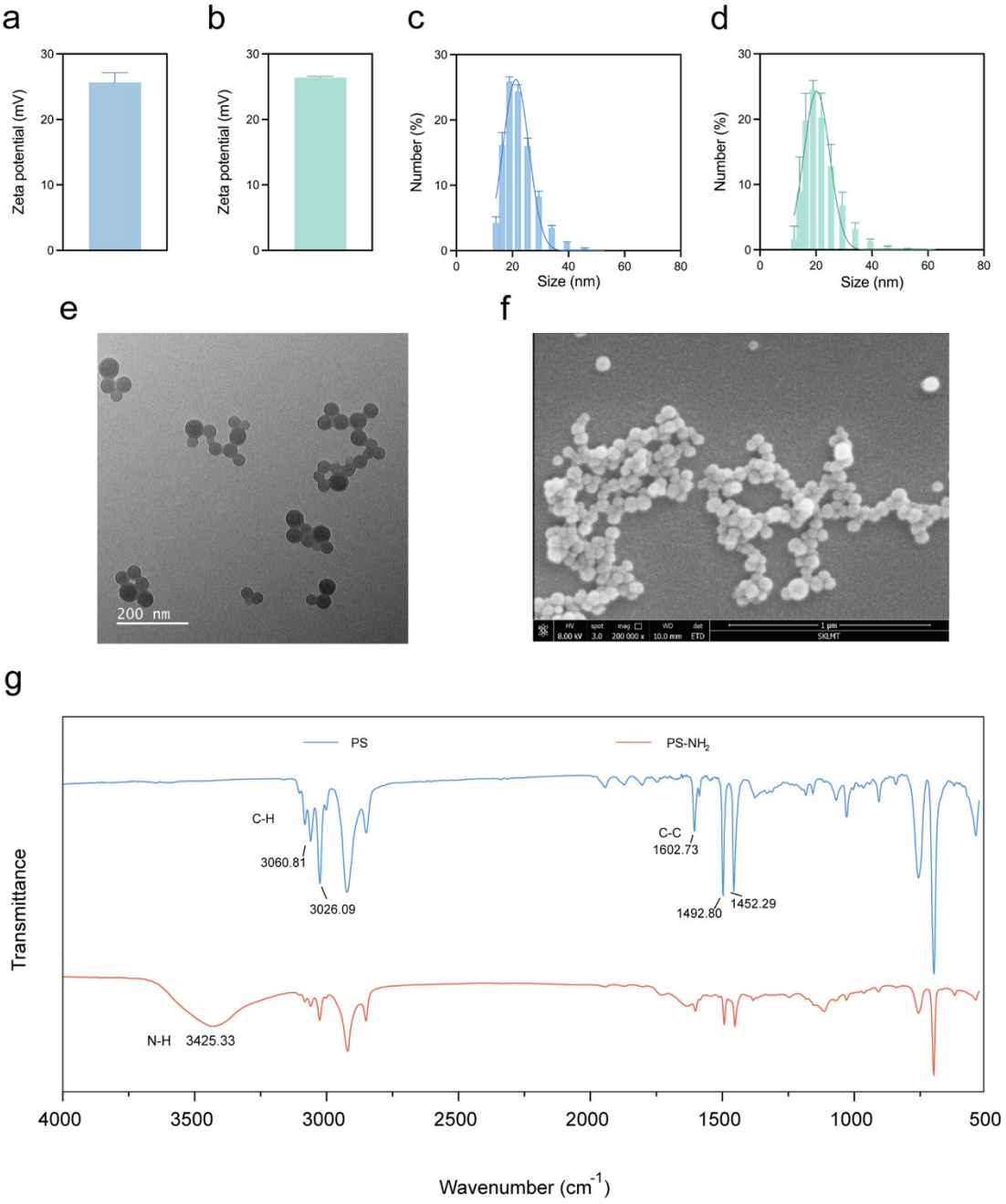

Fig. S1. Characterization of PS-NH_2. Zeta potentials of PS-NH_2 in different matrices: (a): Pure water, (b): BG-11; Corresponding hydrodynamic diameters of PS-NH_2 in different matrices: (c): Pure water, (d): BG-11; SEM images of PS-NH_2 (e); TEM images of PS-NH_2 (f); FTIR of pristine PS MPs and PS-NH_2 (g).

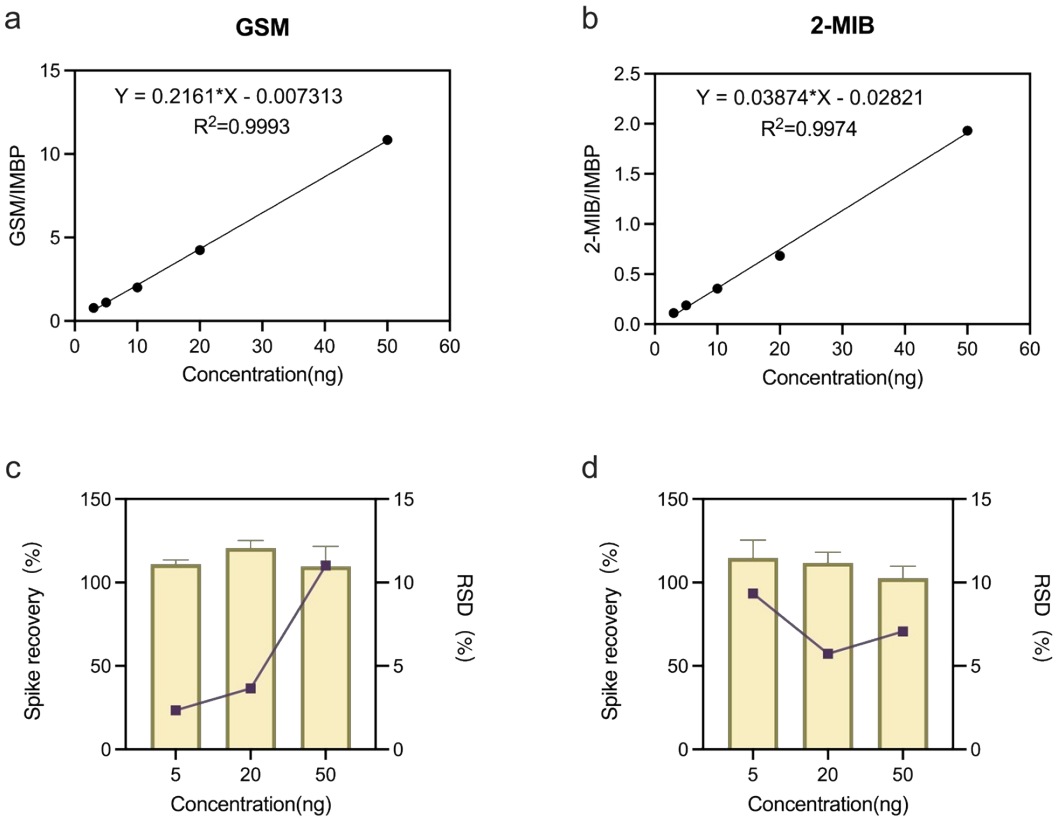

Fig. S2. Analytical method validation for the quantification of GSM and 2-MIB. Calibration curves of GSM (a) and 2-MIB (b) using the internal standard method (IMBP as internal standard). Spike recovery rates (bars, left Y-axis) and relative standard deviations (RSD, lines, right Y-axis) of GSM (c) and 2-MIB(d) at different spiked concentrations (5, 20, and 50 ng).

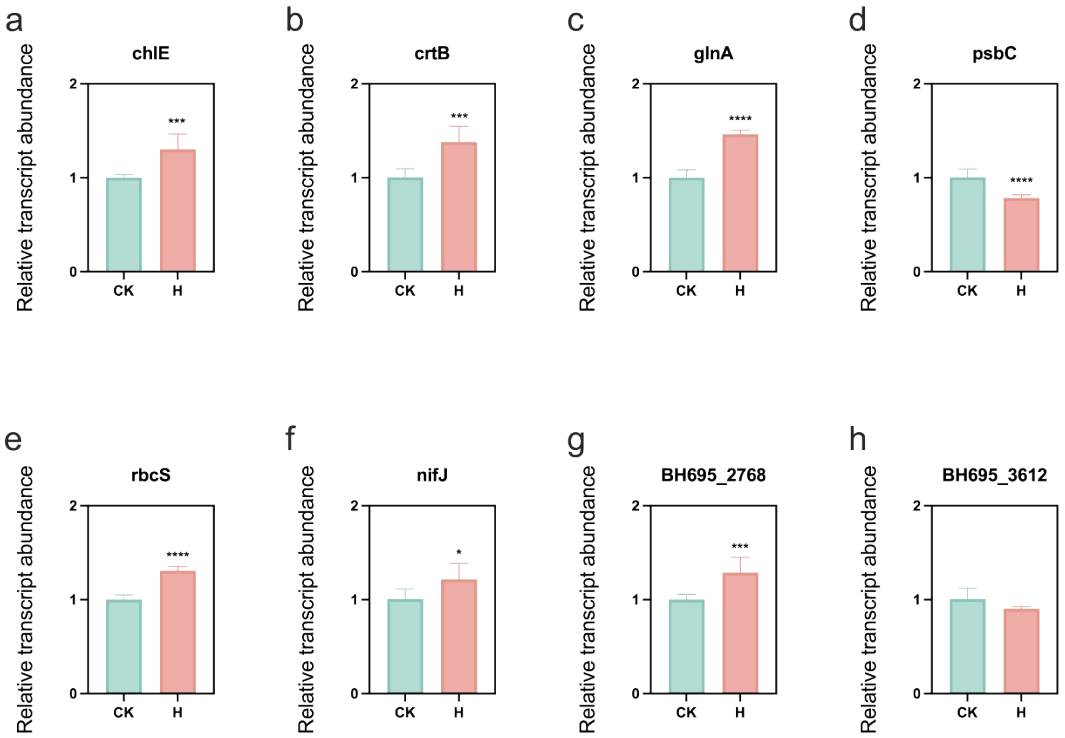

Fig. S3. Relative expression of the related gene of *M. aeruginosa* to PS-NH_2 by qPCR. Magnesium-protoporphyrin IX monomethyl ester (oxidative) cyclase (chlE) (a), 15-cis-phytoene synthase (crtB) (b), glutamine synthetase (glnA) (c), photosystem II CP43 chlorophyll apoprotein (psbC) (d), ribulose-bisphosphate carboxylase small chain (rbcS) (e), pyruvate-ferredoxin/flavodoxin oxidoreductase (nifJ) (f), peroxidase activity (BH695_2768) (g), integral component of membrane (BH695_3612) (h).

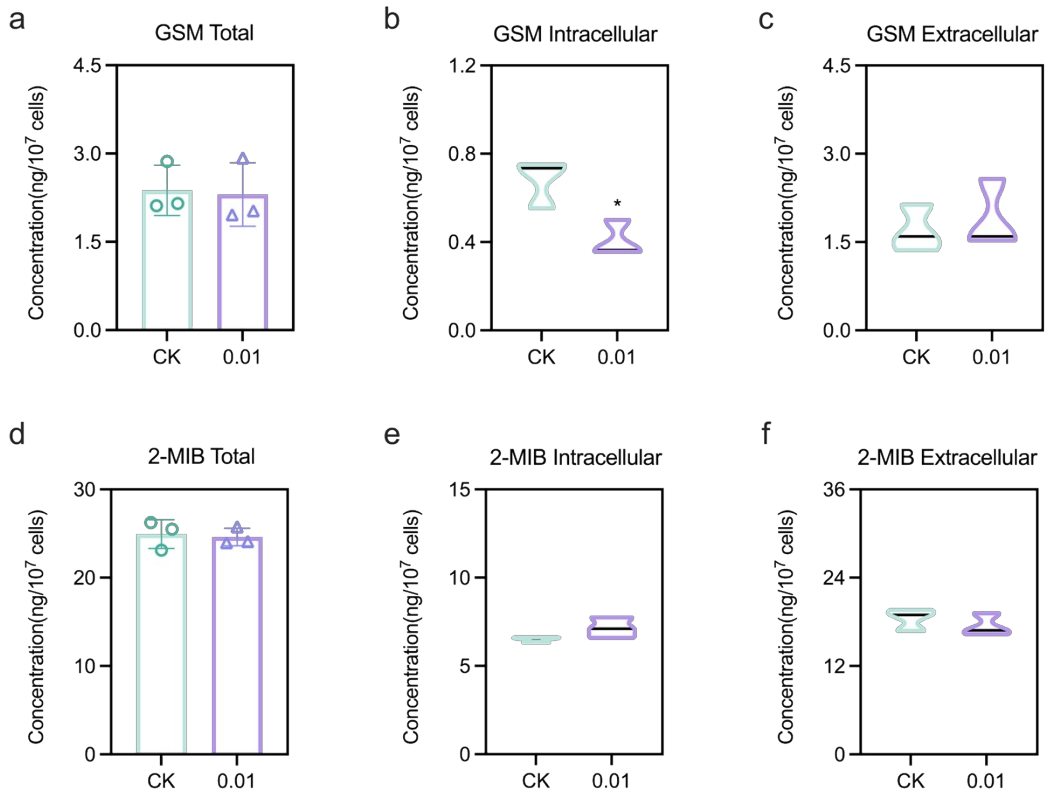

Fig. S4 Effect of different concentrations PS-NH_2 on the production of T&Os in *M. aeruginosa* (control and 0.01 μg/mL). GSM concentrations (total, intracellular, and extracellular): (a, b, c); 2-MIB concentrations (total, intracellular, and extracellular): (d, e, f). *: $p < 0.05$, **: $p < 0.01$, ***: $p < 0.001$, ****: $p < 0.0001$.

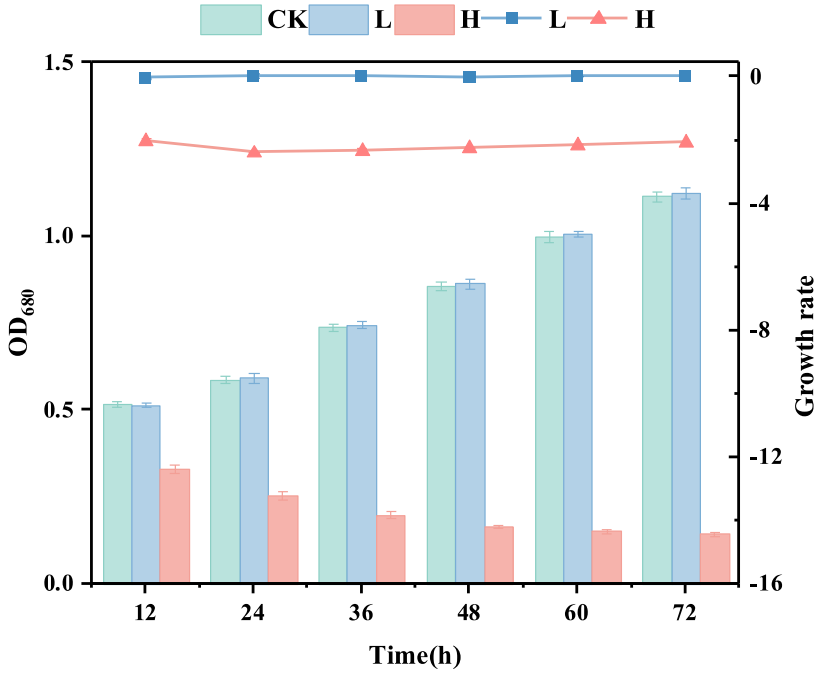

Fig. S5. Changes in growth and growth inhibition rate of *M. aeruginosa* under different concentrations of PS-NH_2 treatment during exposure.

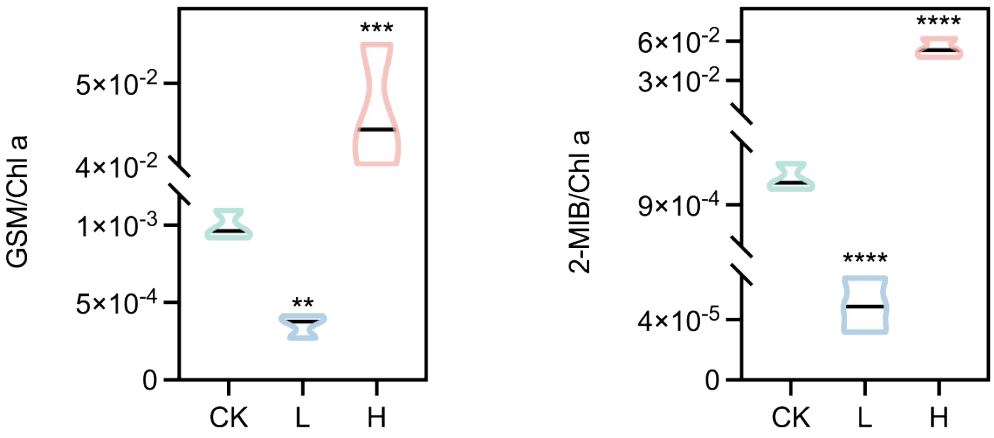

Fig. S6. The T&Os yield per chl *a* production of *M. aeruginosa* under different concentrations PS-NH_2 (a-GSM, B-2-MIB).

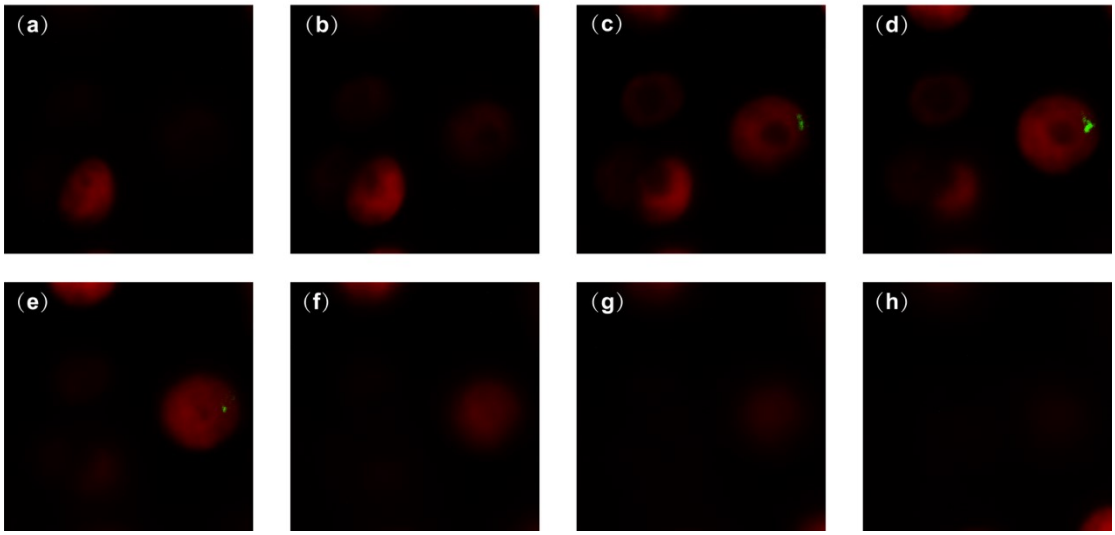

Fig. S7. Laser confocal scanning images of *M. aeruginosa*.

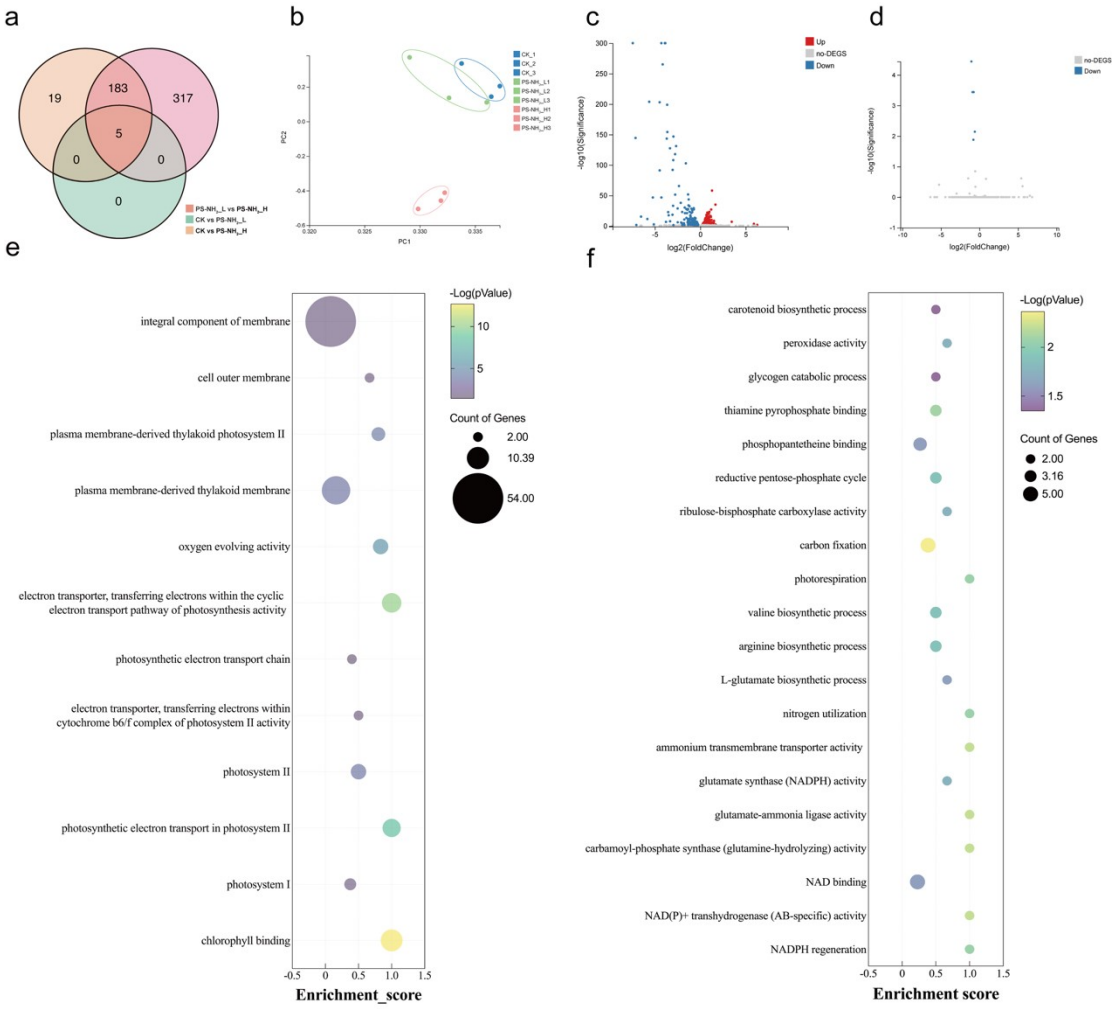

Fig. S8. Transcriptomic analysis of *M. aeruginosa* after 3 days of exposure. Differential gene Venn diagram for the control, 1 μg/mL, and 20 μg/mL PS-NH_2 treatment groups (a); principal component analysis results for different treatment groups (b); number of differential metabolites (c, d); GO enrichment analysis of differentially expressed genes under high-concentration PS-NH_2 and downregulated (e), upregulated (f) pathways.

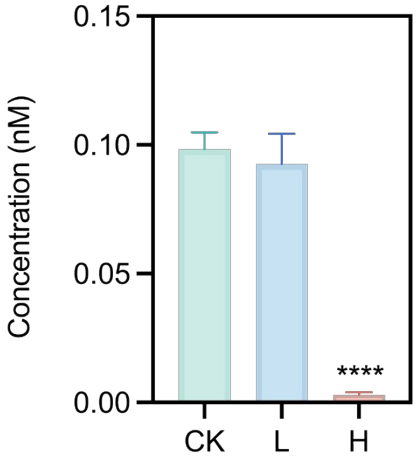

Fig. S9 Inhibitory effects of PS-NH_2 exposure on the intracellular ATP concentration.

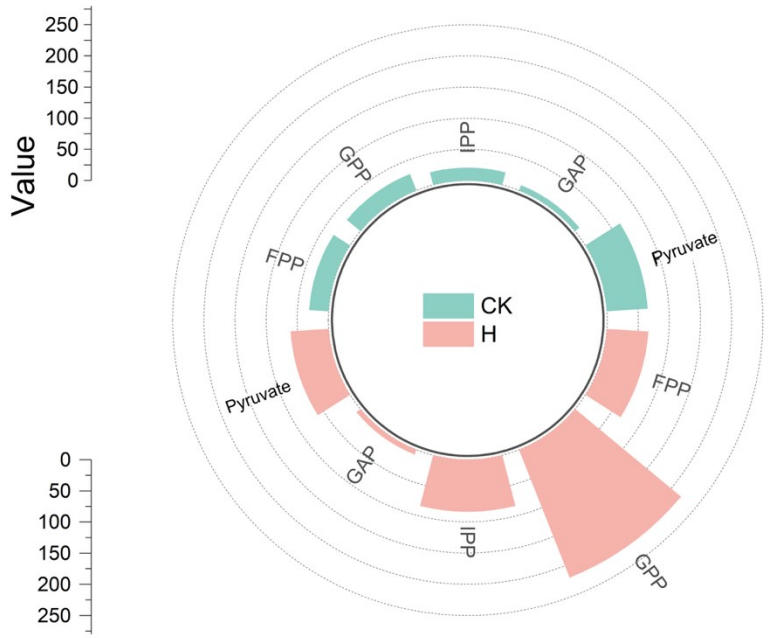

Fig. S10. Changes in the metabolic content of precursor molecules for T&Os synthesis.

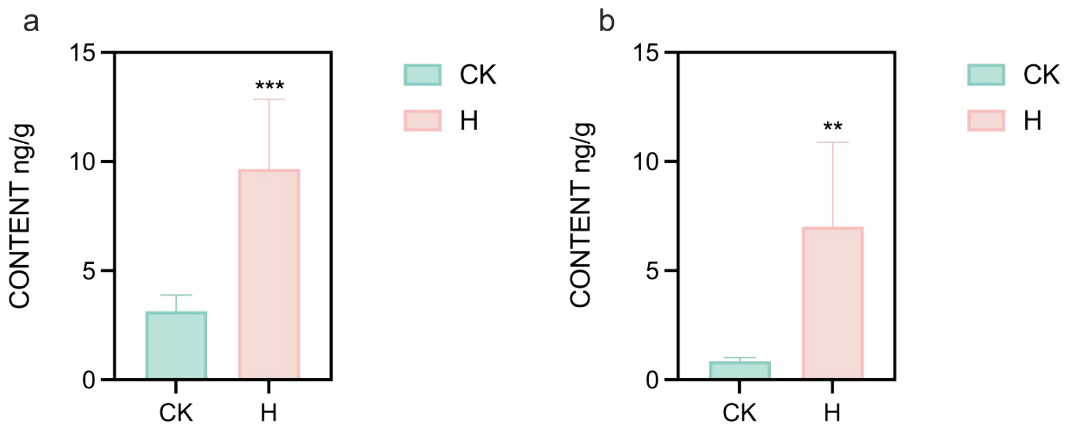

Fig. S11. Changes in T&Os metabolite content (a-GSM, b-2-MIB).

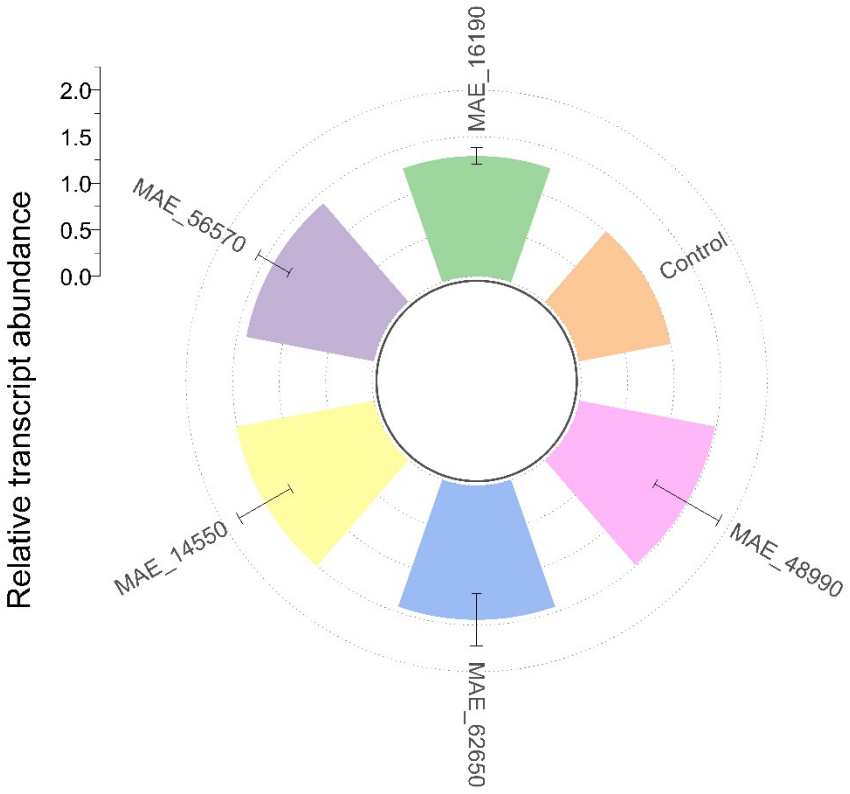

Fig. S12. Changes in the expression of key enzyme genes in the synthesis pathways of key precursor molecules for T&Os synthesis.

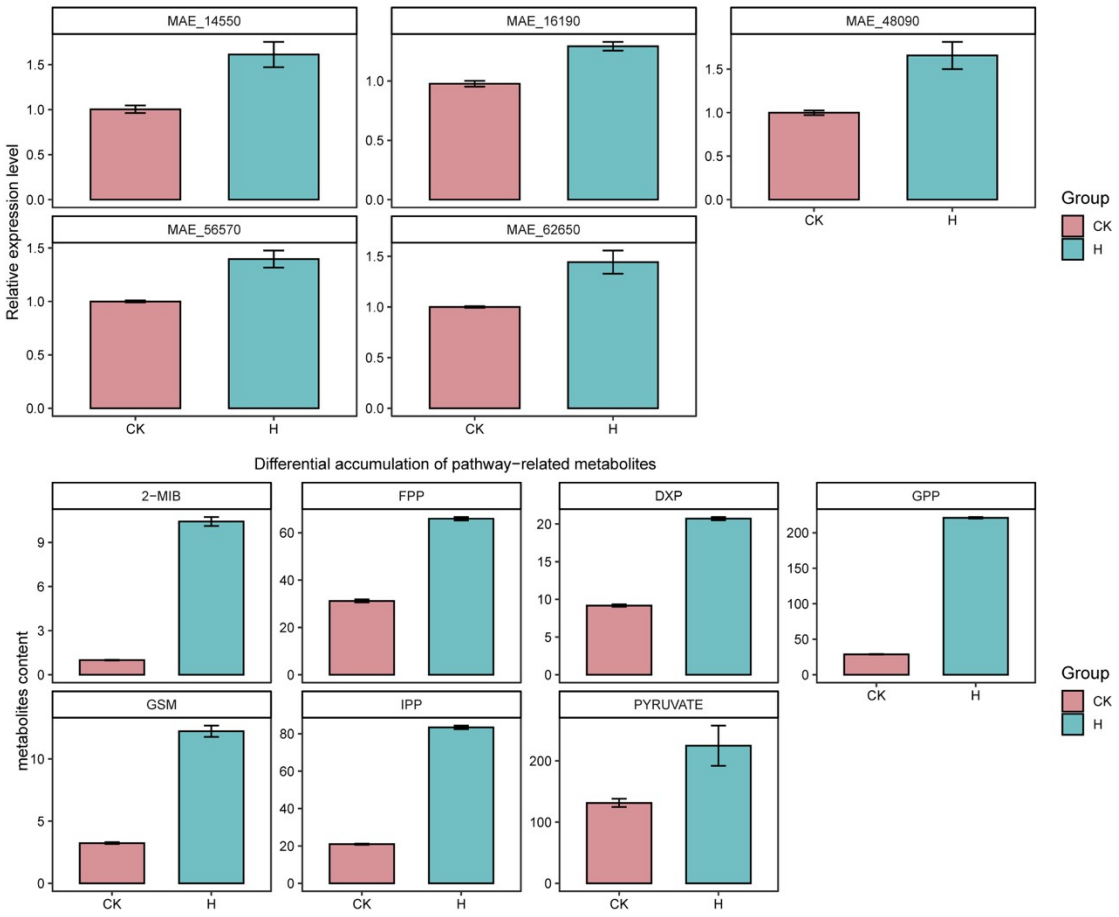

Fig. S13. Differential expression of pathway-related genes. Differential expression of pathway − related genes (a); differential accumulation of pathway−related metabolite (b).

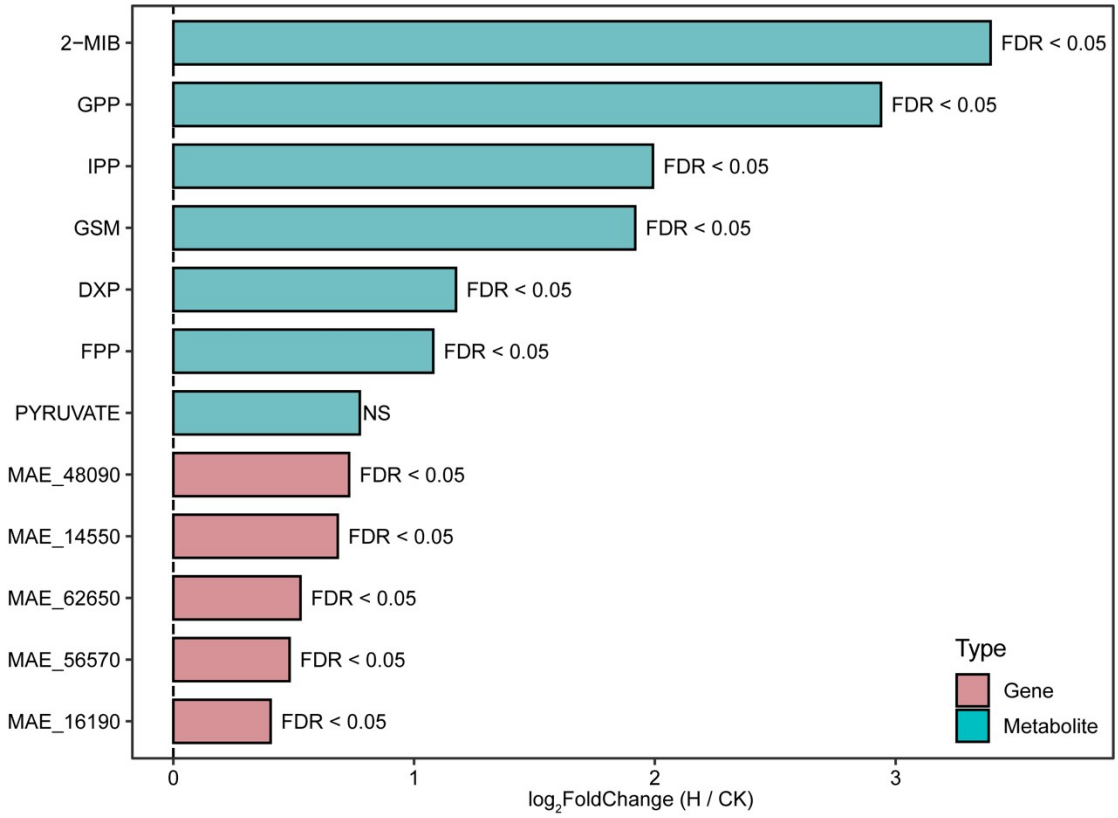

Fig. S14 Variation trends of genes and metabolites.

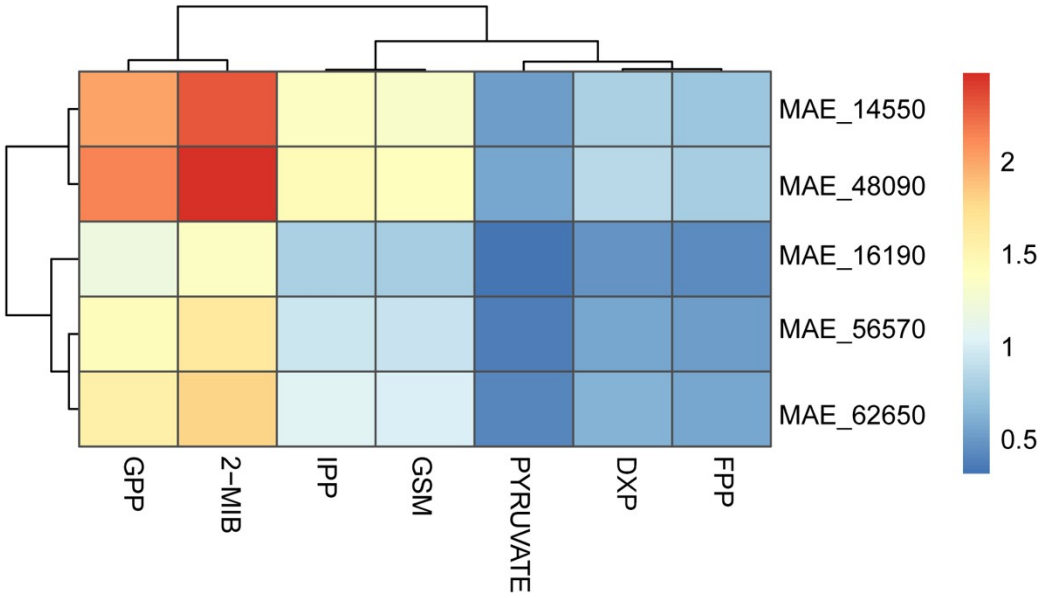

Fig. S15 Trend association between genes and metabolites.

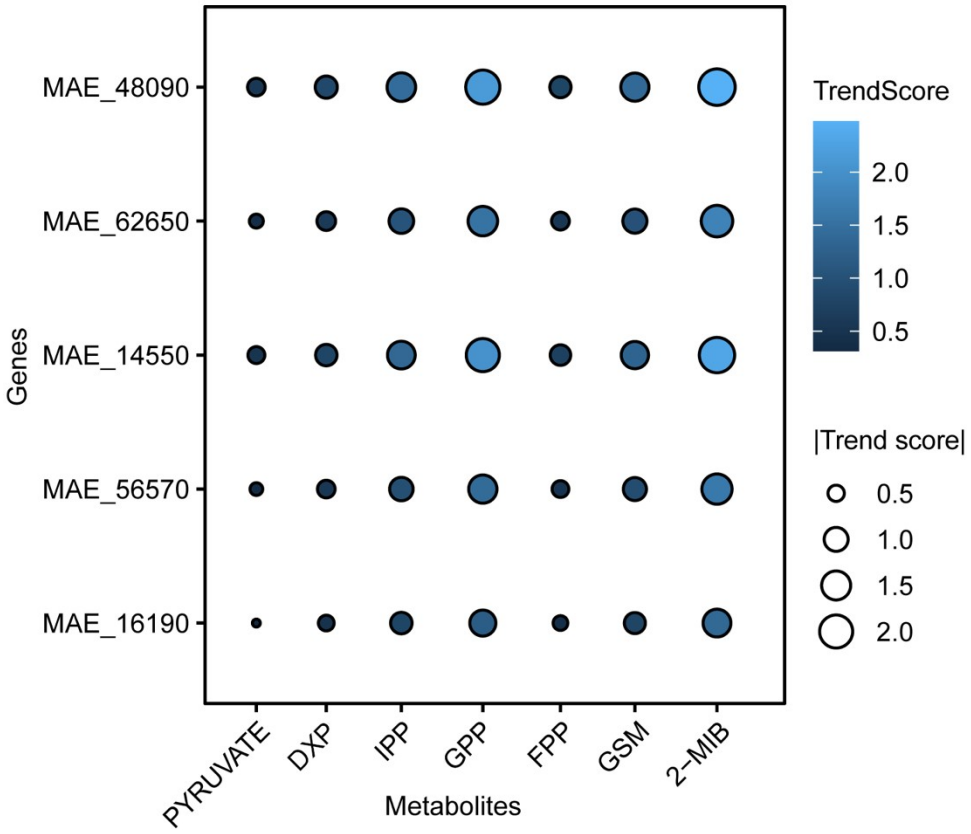

Fig. S16 Gene-metabolite trend association.

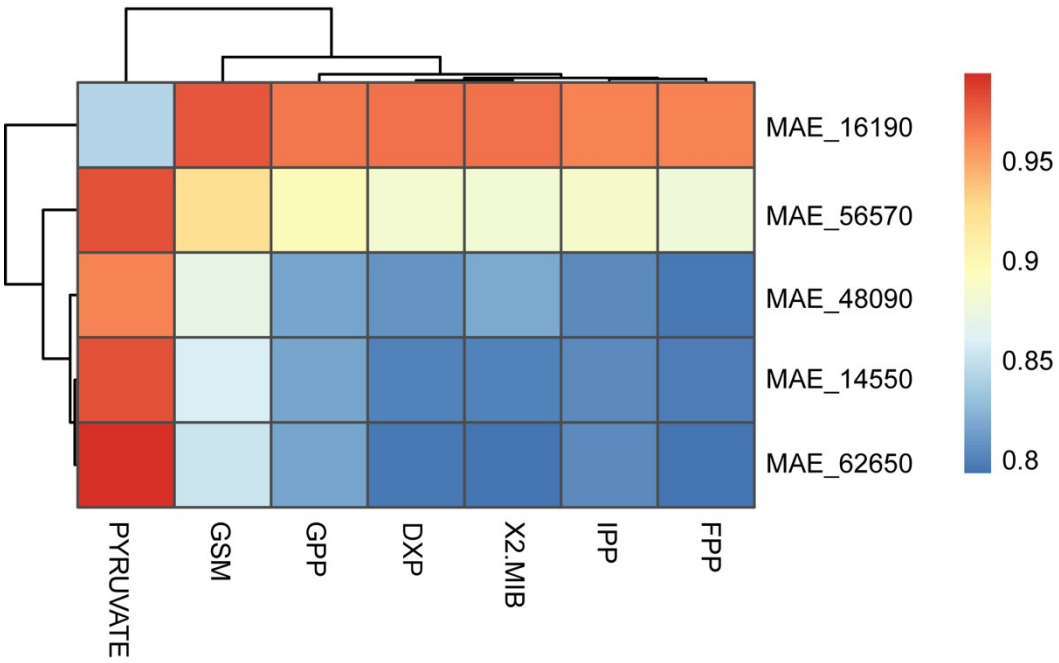

Fig. S17 Exploratory correlation between genes and metabolites.

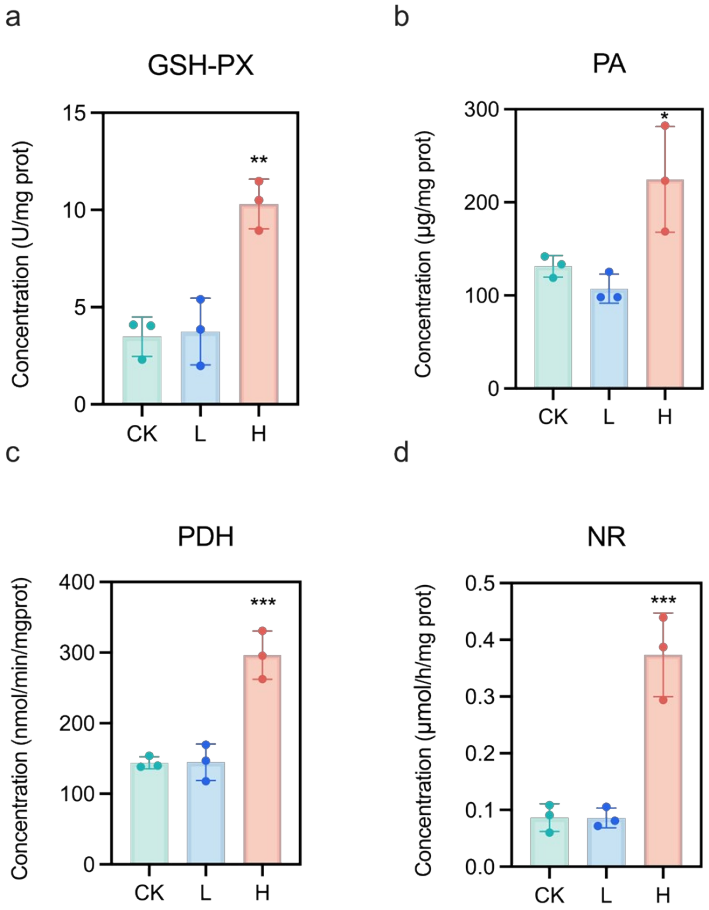

Fig. S18. Biochemical responses of *M. aeruginosa* under different PS-NH_2 treatments. Changes in GSH-PX activity (a), PA (b), PDH activity (c), and NR activity (d). $p < 0.01$, ***: $p < 0.001$, ****: $p < 0.0001$.

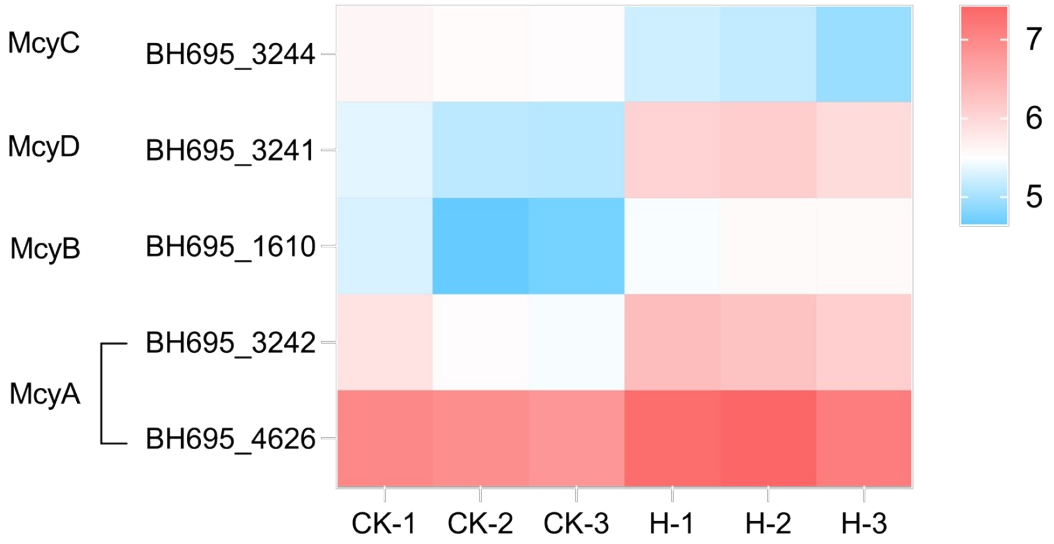

Fig. S19. Heatmap of the genes expression of microcystin synthetase protein genes in *M. aeruginosa* treated with PS-NH_2.

Reference

1. Q. Xie, R. Gu, D. Lin, N. Liu, R. Qu and F. Ge, Environ. Sci. Technol., 2022, 56, 13066-13075.